九州大学学術情報リポジトリ
Kyushu University Institutional Repository

Prediction of the Stiffness and Stresses for Carbon Nano-Tube Composites Based on Homogenization Analysis

Luo, Dong-Mei.
Research Institute for Applied Mechanics, Kyushu University

Wang, Wen-Xue
Research Institute for Applied Mechanics, Kyushu University

Takao, Yoshihiro
Research Institute for Applied Mechanics, Kyushu University

Kakimoto, Koichi
Research Institute for Applied Mechanics, Kyushu University

https://doi.org/10.15017/26794

出版情報：九州大学応用力学研究所所報. 129, pp.37-45, 2005-09. Research Institute for Applied Mechanics, Kyushu University
バージョン：
権利関係：

Prediction of the Stiffness and Stresses for Carbon Nano-Tube Composites Based on Homogenization Analysis

Dong-Mei. LUO[*1], Wen-Xue WANG[*1], Yoshihiro TAKAO[*1] and Koichi KAKIMOTO[*1]

E-mail of corresponding author: *bungaku@riam.kyushu-u.ac.jp*

(Received July 29, 2005)

Abstract

Numerical prediction of the macroscopic stiffness and microscopic stresses for carbon nanotube polymer composites is performed based on the homogenization theory. A new solution method is proposed for the homogenization analysis. The conventional inhomogeneous integral equation related to the microscopic mechanical behavior in the basic unit cell is replaced by a homogeneous integral equation based on a new characteristic function. According to the new solution method, the computational problem of the characteristic function subject to initial strains and periodic boundary conditions is reduced to a simple displacement boundary value problem without initial strains, which simplifies the computational process. The effects of various geometry parameters including straight and wavy nanotubes on the macroscopic stiffness and microscopic stresses are presented. Numerical results are compared with previous results obtained from the Halpin-Tsai equations, Mori-Tanaka method, which proves that the present method is valid and efficient.

Key words : Carbon nanotube composite, Homogenization theory, Solution method, Macroscopic Stiffness, Microscopic stresses

1. Introduction

The extremely high strength and stiffness combining with high aspect ratio make carbon nanotube (CNT) become attractive as reinforcement of polymer matrix composites. Many researches of experimental and analysis have been carried to develop CNT polymer composites, e.g. as reviewed by Andrews and Weisenberger [1]. In order to promote the development of excellent CNT ploymer composites, the prediction of the macroscopic stiffness and microscopic stresses plays an important role in the design and the application of CNT ploymer composites in practice. On the other hand, it is extremely difficult to analyze a CNT polymer composite with complex material heterogeneity involving with individual nanotubes precisely due to the huge computational time and cost. Hence, many researches have been focused on exploring an approximate but simple and efficient analysis method.

Halpin-Tsai equation [2] is a popular method for predicting the macroscopic properties of traditional fiber-reinforced composites. The modified Halpin-Tsai equation is utilized to predict the elastic properties of CNT polymer composites in [3]. Mori-Tanaka method developed in (e.g. [4,5]) is also a well-known method to predict the macroscopic material properties of various composites and is applied to the prediction of macroscopic stiffness of nano-composites with layered silicate [6] and long wavy CNT polymer composites[7]. However, both of these two methods have a common shortcoming that they cannot accurately reflect the interactions between neighboring fibers or nanotubes because of the limitation of their analytical models. Recently, a shear lag model is developed to study the macroscopic stiffness [8]. It is a very simple analysis, but it also cannot reflect the interactions between neighboring nanotubes accurately.

In parallel to the above analytical methods, different approaches to composites analysis have been also developed based on the analysis of a basic cell by finite element method (FEM) in the past years. In general, these approaches can be roughly classified into the average-field method and the homogenization method. The average-field method (e.g. [9]) has been developed based on the physical viewpoint that the macroscopic material properties obtained from experiments represent the properties of volume average. In contrast, the homogenization method (e.g. [10]) has been developed based on the mathematically multi-scale perturbation theory. In [7,11], the average-field method is used to

*1 Research Institute for Applied Mechanics, Kyushu University

predict the macroscopic properties of straight CNT and long wavy CNT polymer composites. However, it is realized that it is difficult to impose exact periodic condition along a basic unit cell with asymmetric and complicated microstructures in the average-field method [12]. In the case of homogenization method, a characteristic function of the third order tensor is introduced to relate the microscopic displacements to the macroscopic displacements, which make it possible to express the exact periodic conditions formally along the boundary of a basic cell. However, since the integral equation related to the characteristic function is inhomogeneous, two computational processes of imposing initial strains and periodic displacement conditions are needed to obtain the characteristic function in the conventional solution method. It is obviously inefficient because there are six independent sets of components of the characteristic function need to be solved for a general three-dimensional unit cell.

In this paper, numerical predictions of the macroscopic stiffness and microscopic stresses for CNT polymer composites are performed based on the homogenization theory. A new solution method is proposed for the homogenization analysis. According to the new solution method, the computational problem of the characteristic function subject to initial strains and periodic boundary conditions is reduced to a simple displacement boundary value problem without initial strains, which simplifies the computational process. The effects of various geometry parameters including straight and wavy nanotubes on the macroscopic stiffness and microscopic stresses are presented. Numerical results are compared with previous results obtained from the Halpin-Tsai equations, Mori-Tanaka method.

2. Formulation

Consider a linearly elastic body with a periodic microstructure, as shown in Fig. 1. Ω denotes the open subset of three-dimensional space occupied by the body, Γ the boundary of Y the open subset of the space occupied by the basic unit cell, S_Y the boundary of Y. The sub-domain Y_2 may represent an inclusion in the unit cell to describe a composite, or a void to describe a porous material. Define S_{y12} as the interface when Y_1 and Y_2 are different materials, or as the internal boundary of Y_1 when Y_2 represents a void. For the sake of simplicity, it is assume that S_{Y12} is a traction-free surface if Y_2 represents a void. A brief review of the basic equations of homogenization theory is given in the following paragraphs.

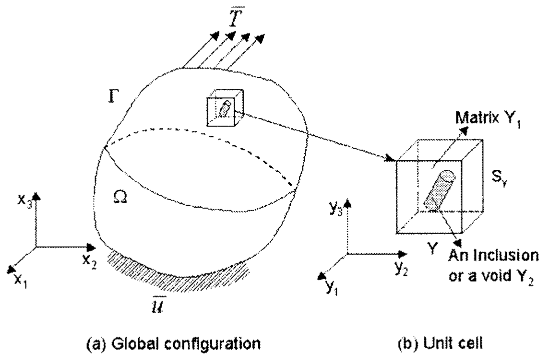

Fig.1 A material with periodic microstructures.

In the construction of the homogenization theory, the displacements $u_i(\mathrm{x})$ are assumed as an asymptotic expansion with respect to a parameter η that is a scaling factor of the microscopic/macroscopic dimension, i.e.

$$u_i(\mathrm{x}) = u_i^0(\mathrm{x},\mathrm{y}) + \eta u_i^1(\mathrm{x},\mathrm{y}) + \eta^2 u_i^2(\mathrm{x},\mathrm{y}) + \cdots \quad (1)$$

Where $\mathrm{x} = (x_1, x_2, x_3)$ and $\mathrm{y} = (y_1, y_2, y_3)$ represent the macroscopic and the microscopic coordinate systems, respectively, which are related to each other by

$$y_i = \frac{x_i}{\eta} \quad (2)$$

Then, based on the elasticity, the strain-displacement and stress-strain relations can be expressed as

$$\varepsilon_{ij} = \frac{1}{2}\left(\frac{\partial u_i}{\partial x_j} + \frac{\partial u_j}{\partial x_i}\right), \quad \sigma_{ij} = E_{ijkl}\varepsilon_{kl} \quad (3)$$

Where E_{ijkl} denotes the elastic constants tensor. Applying the chain rule of differentiation of a function with implicit variables to the partial differentials of (3) leads to

$$\varepsilon_{ij} = \frac{1}{2\eta}\left(\frac{\partial u_i^0}{\partial y_j} + \frac{\partial u_j^0}{\partial y_i}\right) + \frac{1}{2}\left[\left(\frac{\partial u_i^0}{\partial x_j} + \frac{\partial u_j^0}{\partial x_i}\right) + \left(\frac{\partial u_i^1}{\partial y_j} + \frac{\partial u_j^1}{\partial y_i}\right)\right] + \frac{\eta}{2}\left[\left(\frac{\partial u_i^1}{\partial x_j} + \frac{\partial u_j^1}{\partial x_i}\right) + \left(\frac{\partial u_i^2}{\partial y_j} + \frac{\partial u_j^2}{\partial y_i}\right)\right] + \cdots \quad (4)$$

$$\sigma_{ij} = \frac{1}{\eta}E_{ijkl}\frac{\partial u_k^0}{\partial y_l} + E_{ijkl}\left(\frac{\partial u_k^0}{\partial x_l} + \frac{\partial u_k^1}{\partial y_l}\right) + \eta E_{ijkl}\left(\frac{\partial u_k^1}{\partial x_l} + \frac{\partial u_k^2}{\partial y_l}\right) + \cdots \quad (5)$$

According to the elasticity, the virtual displacement equation can be expressed as:

$$\int_\Omega E_{ijkl}\frac{\partial u_k}{\partial x_l}\frac{\partial v_i}{\partial x_j}d\Omega = \int_\Omega f_i v_i d\Omega + \int_{\Gamma_T} \bar{T}_i v_i d\Gamma \quad (6)$$

Where Γ_T denotes the region of the boundary Γ with specified tractions $\bar{T}_i$, v_i is the virtual displacement and $v_i = 0$ on the Γ_u where $u_i = \bar{u}_i$, f_i is the body force. By inserting (1) into the above virtual displacement equation, applying the chain rule of differentiation to the partial differentials of u_k and v_i, and equating the terms with the same power of η, we can derive a series of equations related to the displacements u_i^0, u_i^1, u_i^2 and so on as follows.

$$u_i^0(\mathrm{x},\mathrm{y})=u_i^0(\mathrm{x}) \tag{7}$$

$$\int_Y E_{ijkl}\left(\frac{\partial u_k^0(\mathrm{x})}{\partial x_l}+\frac{\partial u_k^1(\mathrm{x},\mathrm{y})}{\partial y_l}\right)\frac{\partial v_i(\mathrm{y})}{\partial y_j}dY=0 \qquad v_i\in Y \tag{8}$$

$$\int_\Omega \left[\frac{1}{|Y|}\int_Y E_{ijkl}\left(\frac{\partial u_k^0(\mathrm{x})}{\partial x_l}+\frac{\partial u_k^1(\mathrm{x},\mathrm{y})}{\partial y_l}\right)dY\right]\frac{\partial v_i(\mathrm{x})}{\partial \mathrm{x}_j}d\Omega$$

$$=\int_\Omega \left(\frac{1}{|Y|}\int_Y f_i dY v_i(\mathrm{x})d\Omega+\int_{\Gamma_t}\bar{T}_i v_i(\mathrm{x})d\Gamma \qquad v_i\in\Omega \tag{9}$$

$$\int_Y E_{ijkl}\left(\frac{\partial u_k^1(\mathrm{x})}{\partial x_l}+\frac{\partial u_k^2(\mathrm{x},\mathrm{y})}{\partial y_l}\right)\frac{\partial v_i(\mathrm{y})}{\partial y_j}dY$$

$$=\int_Y f_i v_i(\mathrm{y})dY \qquad v_i\in Y \tag{10}$$

...

etc.

Theoretically, solving all the above equations together with specified boundary conditions will yields the full solution for u_i^0, u_i^1, $u_i^2,\cdots$. However, the first order approximation of $u_i(\mathrm{x})$ is usually of interest for many practical applications. Then only two equations of (8) and (9) related to u_i^0 and u_i^1 need to be solved.

In the conventional solution method for the homogenization analysis, it is assumed that

$$u_k^1(\mathrm{x},\mathrm{y})=-\chi_k^{pq}(\mathrm{x},\mathrm{y})\frac{\partial u_p^0(\mathrm{x})}{\partial x_q}+\tilde{u}_k^1(\mathrm{x}) \tag{11}$$

Where χ_k^{pq}, called as characteristic function, is an unknown Y- periodic tensor of the third order. It is noted that χ_k^{pq} may also be considered as a symmetric tensor of the second order for each k (k=1,2,3). Inserting (11) into (8) leads to

$$\int_Y E_{ijpq}\frac{\partial \chi_p^{kl}(\mathrm{x},\mathrm{y})}{\partial y_q}\frac{\partial v_i(\mathrm{y})}{\partial y_j}dY=\int_Y E_{ijkl}\frac{\partial v_i(\mathrm{y})}{\partial y_j}dY \tag{12}$$

$$(y_1,y_2,y_3)\Big|_{\substack{face1\\face3}}=(\mp\frac{a}{2},y_2,y_3)$$

$$(y_1,y_2,y_3)\Big|_{\substack{face2\\face4}}=(y_1,\mp\frac{b}{2},y_3)$$

$$(y_1,y_2,y_3)\Big|_{\substack{face5\\face6}}=(y_1,y_2,\mp\frac{c}{2}) \tag{13}$$

Then the periodic boundary conditions of $u_k^1(\mathrm{x},\mathrm{y})$ require

$$u_k^1(\mathrm{x},\mathrm{y})\big|_{face1}=u_k^1(\mathrm{x},\mathrm{y})\big|_{face3}$$

$$u_k^1(\mathrm{x},\mathrm{y})\big|_{face2}=u_k^1(\mathrm{x},\mathrm{y})\big|_{face4}$$

$$u_k^1(\mathrm{x},\mathrm{y})\big|_{face5}=u_k^1(\mathrm{x},\mathrm{y})\big|_{face6} \tag{14}$$

Inserting (11) into the above equations leads to

$$-\chi_k^{pq}(\mathrm{x},\mathrm{y})\big|_{face1}=-\chi_k^{pq}(\mathrm{x},\mathrm{y})\big|_{face3}$$

$$-\chi_k^{pq}(\mathrm{x},\mathrm{y})\big|_{face2}=-\chi_k^{pq}(\mathrm{x},\mathrm{y})\big|_{face4}$$

$$-\chi_k^{pq}(\mathrm{x},\mathrm{y})\big|_{face5}=-\chi_k^{pq}(\mathrm{x},\mathrm{y})\big|_{face6} \tag{15}$$

Hence, the characteristic function can be completely determined from (12) and (15).

On the other hand, inserting (11) into (9) leads to

$$\int_\Omega D_{ijkl}^H(\mathrm{x})\frac{\partial u_k^0(\mathrm{x})}{\partial x_l}\frac{\partial v_i(\mathrm{x})}{\partial x_j}d\Omega=\int_\Omega b_i(\mathrm{x})v_i(\mathrm{x})d\Omega$$

$$+\int_{\Gamma_t}\bar{T}_i(\mathrm{x})v_i(\mathrm{x})d\Gamma, \qquad \mathrm{x}\in\Omega \tag{16}$$

$$D_{ijkl}^H(\mathrm{x})=\frac{1}{|Y|}\int_Y\left(E_{ijkl}-E_{ijpq}\frac{\partial \chi_p^{kl}}{\partial y_q}\right)dY \tag{17}$$

$$b_i(\mathrm{x})=\frac{1}{|Y|}\int_Y f_i(\mathrm{x},\mathrm{y})dY \tag{18}$$

Equation (16) describes the macroscopic equilibrium. Where D_{ijkl}^H denotes the homogenized stiffness and is usually called as the macroscopic stiffness. Therefore the basic equations of a homogenization problem in the sense of first order approximation are reduced to the integral equation (12) subject to periodic conditions of (15) and the integral equation (16) subject to specified boundary conditions. Both of the integral equations can be solved separately by the use of FEM. We can firstly obtain $\chi_i^{kl}(\mathrm{x},\mathrm{y})$ by solving (12) and then solve (16) to obtain macroscopic $u_k^0(\mathrm{x})$. If only the homogenized elastic constants D_{ijkl}^H is of interest, we can solve (12) and calculate (17) to obtain $\chi_i^{kl}(\mathrm{x},\mathrm{y})$ and D_{ijkl}^H. Hence, solving (12) is an important step in the homogenization analysis.

Equation (16) describes the macroscopic equilibrium. Where D_{ijkl}^H denotes the homogenized stiffness and is usually called as the macroscopic stiffness. Therefore the basic equations of a homogenization problem in the sense of first order approximation are reduced to the integral equation (12) subject to periodic conditions of (15) and the integral equation (16) subject to specified boundary conditions. Both of the integral equations can be solved separately by the use of FEM. We can firstly

obtain $\chi_i^{kl}(\mathrm{x},\mathrm{y})$ by solving (12) and then solve (16) to obtain macroscopic $u_k^0(\mathrm{x})$. If only the homogenized elastic constants D_{ijkl}^H is of interest, we can solve (12) and calculate (17) to obtain $\chi_i^{kl}(\mathrm{x},\mathrm{y})$ and D_{ijkl}^H. Hence, solving (12) is an important step in the homogenization analysis.

$$\tilde{\chi}_k^{pq}(\mathrm{x},\mathrm{y}) = \chi_{0k}^{pq}(\mathrm{y}) - \chi_k^{pq}(\mathrm{x},\mathrm{y}) \tag{19}$$

Where χ_{0k}^{pq} is also a symmetric tensor of the second order for each k (k=1,2,3) and is expressed by

$$\chi_{0k}^{pq} = \frac{1}{2}(\delta_{pk} y_q + \delta_{qk} y_p) \tag{20}$$

The symbol δ_{ij} is the Kronecker delta. Then the derivation of χ_{0k}^{pq} can be expressed by

$$\frac{\partial \chi_{0k}^{pq}}{\partial y_l} = \frac{1}{2}(\delta_{pk}\delta_{ql} + \delta_{qk}\delta_{pl}) \tag{21}$$

Inserting (21) into (12) and using $E_{ijkl} = E_{ijlk}$ lead to

$$\int_Y E_{ijkl} \frac{\partial \tilde{\chi}_k^{pq}(\mathrm{x},\mathrm{y})}{\partial y_l} \frac{\partial v_i(\mathrm{y})}{\partial y_j} dY = 0 \tag{22}$$

Similarly, by the use of (21) the homogenized elastic constants can be rewritten as

$$D_{ijkl}^H(\boldsymbol{x}) = \frac{1}{|Y|}\int_Y (E_{ijkl} - E_{ijpq}\frac{\partial \chi_{0p}^{kl}}{\partial y_q} + E_{ijpq}\frac{\partial \tilde{\chi}_p^{kl}}{\partial y_q}) dY$$

$$= \frac{1}{|Y|}\int_Y E_{ijpq}\frac{\partial \tilde{\chi}_p^{kl}}{\partial y_q} dY \tag{23}$$

Consequently, it is seen that (12) has been transformed into a homogeneous integral equation (22) in terms of the new characteristic function $\tilde{\chi}_i^{kl}(\mathrm{x},\mathrm{y})$. That is, the original problem with initial strains and periodic conditions is reduced to a simple displacement boundary value problem. Hence, the calculation process of imposing the initial stresses is reduced during the solution of every set $(\chi_1^{kl}, \chi_2^{kl}, \chi_3^{kl})$. Furthermore, the periodic conditions for a rectangular parallelepiped unit cell in terms of $\tilde{\chi}_k^{pq}$ can be easily expressed as follows by the substitution of (19) into (15).

$$[\tilde{\chi}_k^{pq}(\mathrm{x},\mathrm{y}) - \chi_{0k}^{pq}(\mathrm{y})]\Big|_{face1} = [\tilde{\chi}_k^{pq}(\mathrm{x},\mathrm{y}) - \chi_{0k}^{pq}(\mathrm{y})]\Big|_{face3}$$

$$[\tilde{\chi}_k^{pq}(\mathrm{x},\mathrm{y}) - \chi_{0k}^{pq}(\mathrm{y})]\Big|_{face2} = [\tilde{\chi}_k^{pq}(\mathrm{x},\mathrm{y}) - \chi_{0k}^{pq}(\mathrm{y})]\Big|_{face4}$$

$$[\tilde{\chi}_k^{pq}(\mathrm{x},\mathrm{y}) - \chi_{0k}^{pq}(\mathrm{y})]\Big|_{face5} = [\tilde{\chi}_k^{pq}(\mathrm{x},\mathrm{y}) - \chi_{0k}^{pq}(\mathrm{y})]\Big|_{face6} \tag{24}$$

3. Calculation Models

In the present numerical analysis, two kinds of regular and staggered CNT arrays are calculated, as shown in Fig. 2. The unit cell with one CNT is used for the regular array and the unit cell with a complete CNT and four quart CNT is used for the staggered array. Furthermore, the CNT in the unit cell may be straight or wavy in order to investigate the effect of the waviness of CNT on the macroscopic stiffness, as listed in Table 1. That is, five models with straight CNT, wavy CNT and mixed CNTs are calculated. The details of geometrical parameters related to neighboring CNT are depicted in Fig. 3. The diameter D of the CNT is taken as an unit, H_f and T_f describe the half of the distance between neighboring CNTs. The waviness of a wavy CNT is expressed by a sinusoidal function

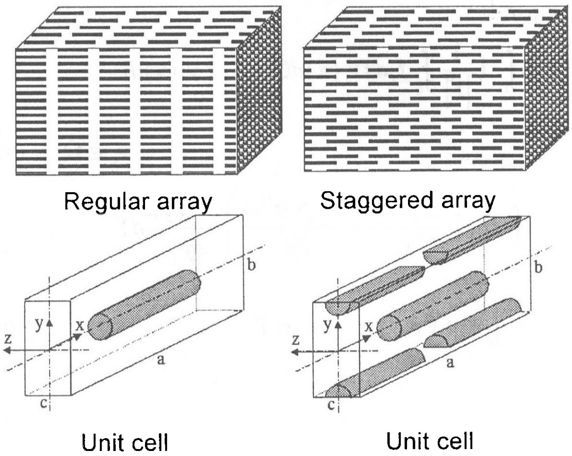

Fig. 2 Two nanotube arrays.

Table 1 Calculation models

Models	Array	Upper CNT	Middle CNT
RS	regular	straight	straight
SS	staggered	straight	straight
RW	regular	wavy	wavy
SW1	staggered	straight	wavy

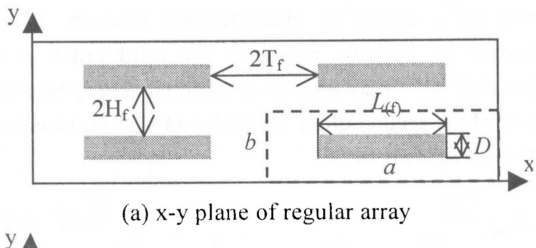

(a) x-y plane of regular array

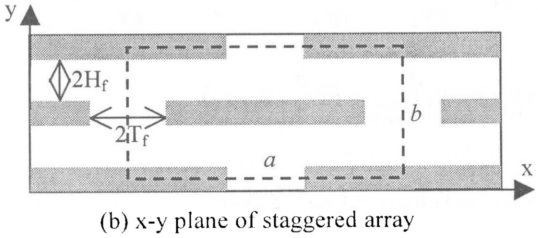

(b) x-y plane of staggered array

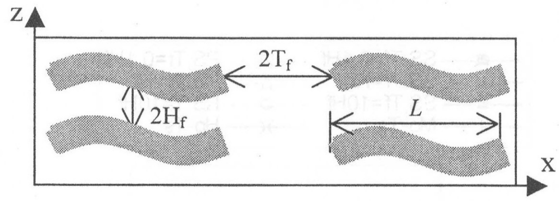

(c) x-z plane of regular array and upper x-z plane of staggered array for wavy CNTs

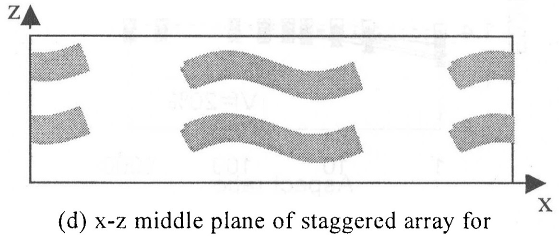

(d) x-z middle plane of staggered array for wavy CNTs

Fig. 3 Geometrical parameters

$$z = A\sin(2\pi x / L) \tag{25}$$

and the wavy plane of the wavy CNT is assumed to coincides with the x-z plane.

4. Numerical Results

In this section, numerical results are presented to demonstrate the validity and efficiency of the new solution method for the prediction of the macroscopic stiffness and microscopic stresses of CNT polymer composites. Finite element analysis is performed by the use of a commercial finite element code ABAQUS. In the calculation, the CNT are considered as a transversely isotropic fiber [13] and the effective stiffness constants are C_{11}=457.6GPa, $C_{12}=C_{13}$=8.4GPa, $C_{22}=C_{33}$=14.3GPa, C_{23}=5.5GPa, $C_{44}=C_{55}$=27.0GPa, and C_{66}==4.4Gpa. The Young's modulus and Poisson's ratio of the matrix are 3.8 GPa and 0.4, respectively.

The variation of macroscopic stiffness with the aspect ratio is shown in Fig. 4 for the case of straight CNTs. Where, SS and RS denote the results of staggered array CNT and regular array CNT, respectively. The results obtained from Mori-Tanaka method and Halpin-Tsai equation are also depicted for a comparison. The ratio of T_f to H_f is taken as a parameter. From these results of four stiffness constants, it is seen that E_{11} is sensitive to the aspect ratio, and that the others are slightly influenced by the aspect ratio, except for small aspect ratio. The staggered array gives high E_{11} than the regular array, especially for relatively large T_f/H_f, but the differences between the two arrays for the other constants are small. The values of E_{11} obtained from Mori-Tanaka method and Halpin-Tsai equation are close to the present ones with T_f=H_f. It is interesting that a small T_f gives high E_{11}, which is useful for the design and fabrication of CNT composites. The present results except for E_{11} predict lower stiffness than Mori-Tanaka method and Halpin-Tsai equation. Figure 5 shows the variation of macroscopic stiffness with the fiber volume fraction. All constants increase with increasing fiber volume fraction. Also only the results for the models with straight CNT are presented. Similarly, a small T_f/H_f gives high E_{11} and the staggered array gives high E_{11} than the regular array, especially for large T_f/H_f.

The effects of waviness of the CNT on the macroscopic stiffness are presented in Fig. 6 and Fig. 7. Figure 6 shows the variations of the stiffness with fiber volume fraction and waviness A/D. It is seen that large waviness reduces E_{11} but improves G_{13} due to the wavy plane coinciding with the x-z plane. The other stiffness constants, that are not presented here, have little variation with the waviness.

The microscopic stresses at the surface of the effective fiber and along the fiber axial direction of the CNT are presented in Fig. 8 when the composite is subjected to a uniform tension. Only two stress components are depicted due to the limitation of pages. The stresses are normalized by the average tensile stress. The upper two figures show the distributions of the fiber axial stress and the shear stress in x-y plane in the case of straight fibers with regular array. The axial stress is almost uniform except for the region near to the two ends, while high shear stress appears in the end regions. These results are similar to the results in many previous papers. The second two figures describe the stress distributions in the case of straight fibers with staggered array. It is seen that high axial stress appears in the middle region due to the influence of neighboring fibers (referring to Fig.3). Also high shear stress occurs in the regions near to the two ends and it is a few higher than that in the case of regular array. The third two figures present the stress distributions in the case of wavy fibers with regular array. The effect of the waviness on the axial stress is apparent and the maximum value occurs at the center region of the fiber, although the variation of the shear stress in x-y plane is not clear. Finally, the lower two figures give the stress distributions in the case of wavy fibers with staggered array. The distribution of the axial stress is similar to that in the case of wavy fibers with regular array, but the variation of the shear stress with the waviness is more obvious. These stress results are useful for the understanding to the microscopic damage and the macroscopic strength of CNT polymer composites.

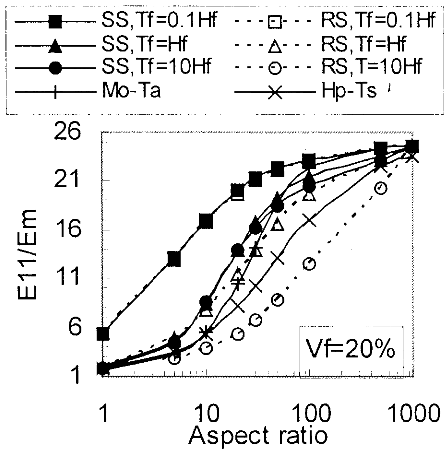

(a) E_{11}/E_m

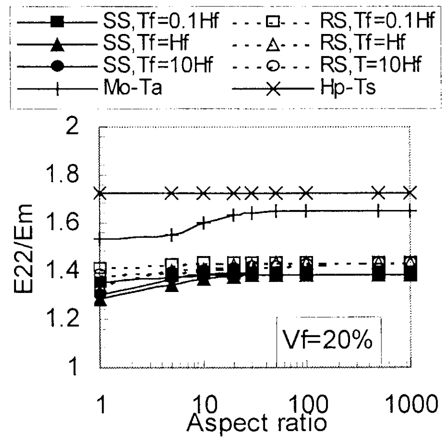

(b) E_{22}/E_m

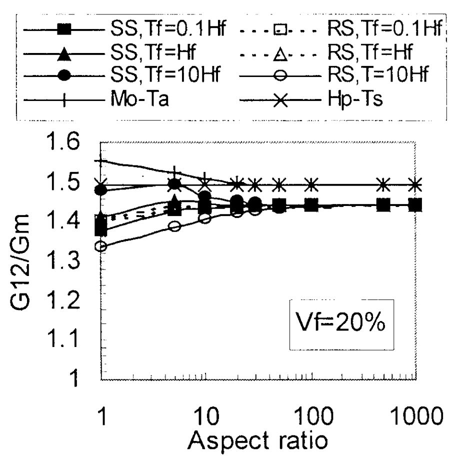

(c) G_{12}/G_m

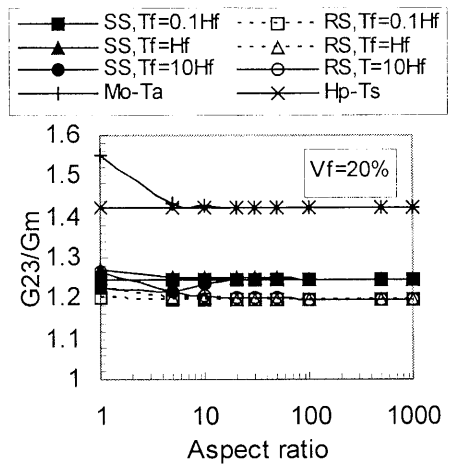

(d) G_{23}/G_m

Fig. 4 Variations of macroscopic stiffness with the fiber aspect ratio.

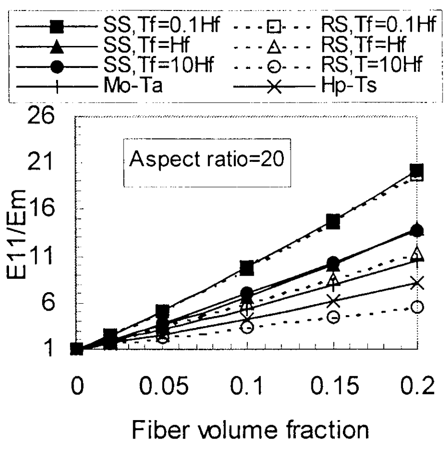

(a) E_{11}/E_m

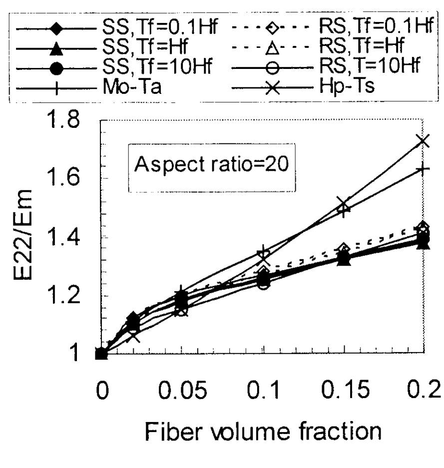

(b) E_{22}/E_m

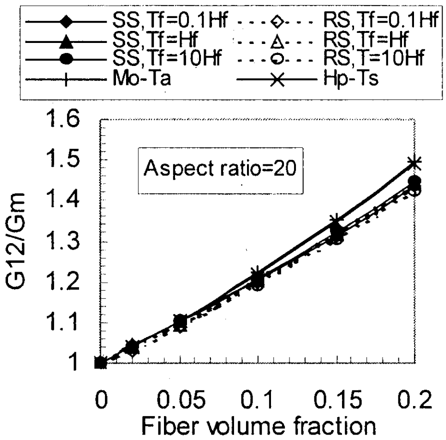

(c) G_{12}/G_m

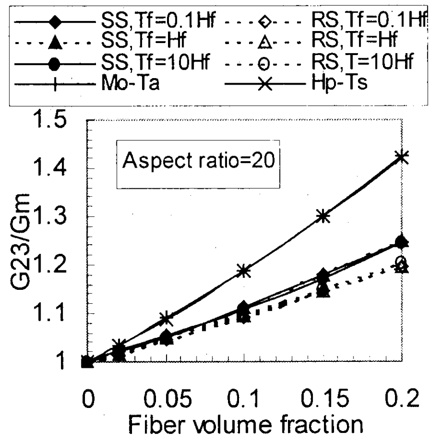

(d) G_{23}/G_m

Fig. 5 Variations of macroscopic stiffness with the fiber volume fraction.

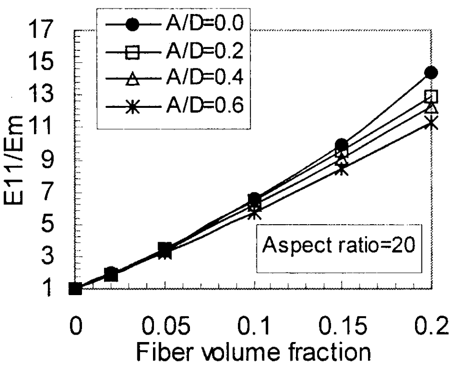

(a) E_{11}/E_m

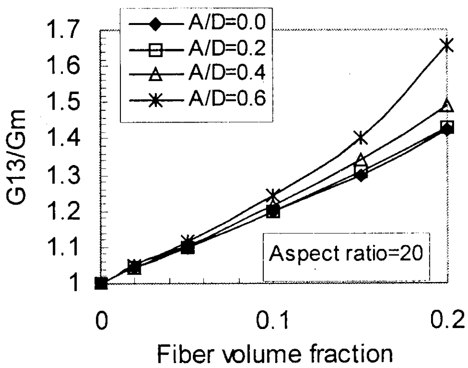

(b) G_{13}/G_m

Fig. 6 Variation of macroscopic stiffness with the fiber volume fraction in the case of SW2 model.

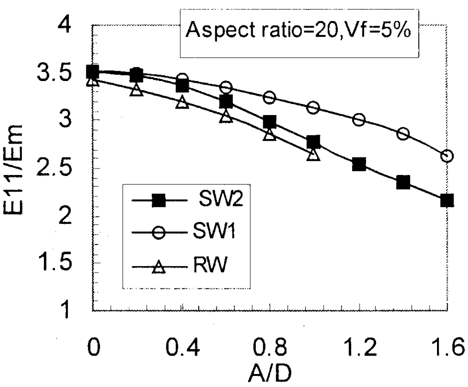

(a) E_{11}/E_m

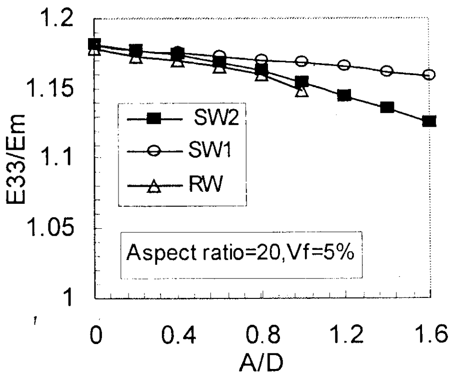

(b) E_{33}/E_m

Fig. 7 Variation of macroscopic stiffness with the waviness of CNTs.

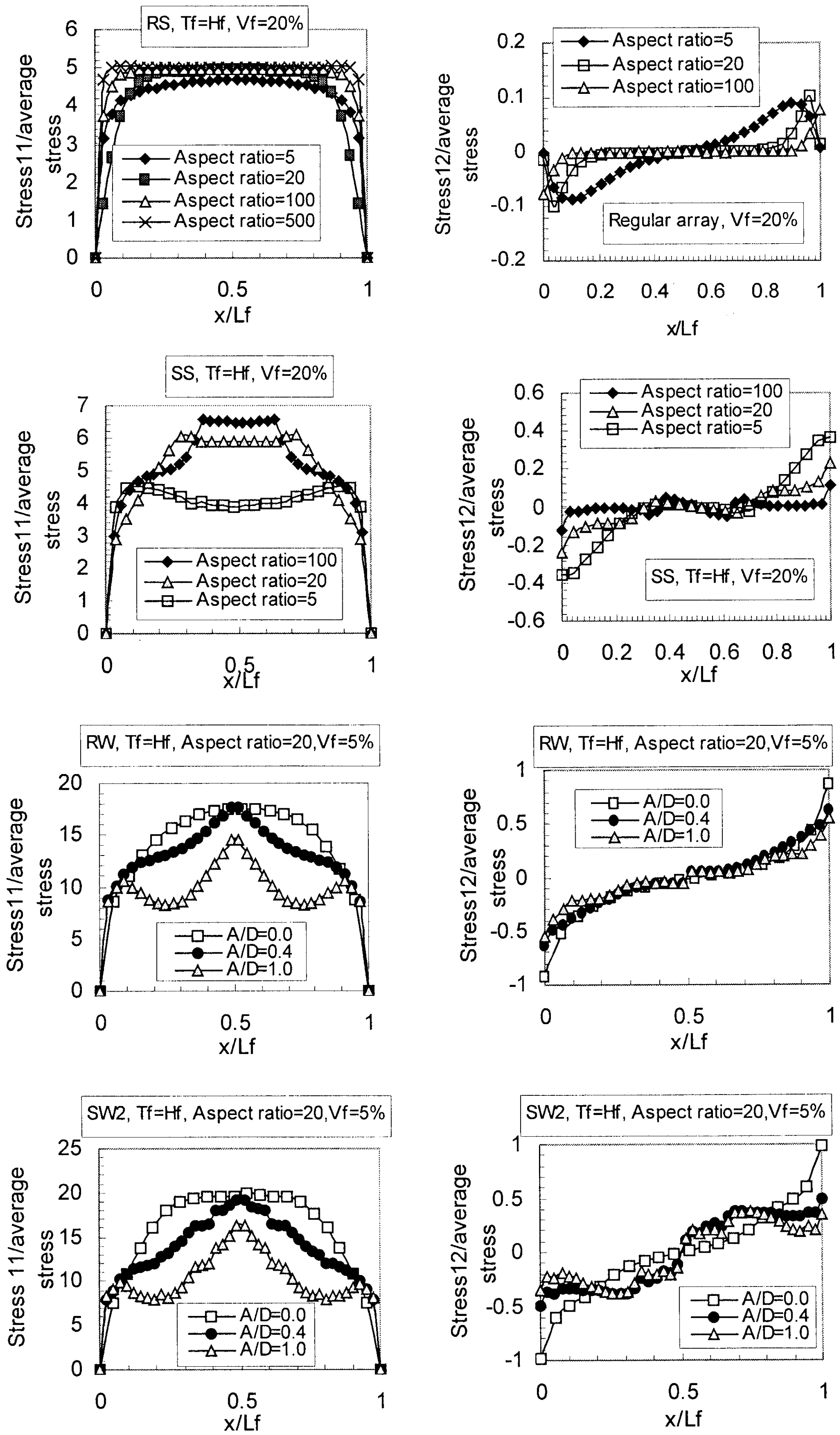

Fig. 8 Microscopic stresses along the effective fiber of the CNT.

5. Summary

A new solution method is proposed for the homogenization analysis. Numerical prediction of the macroscopic stiffness and microscopic stresses for CNT polymer composites is performed based on the new solution method. The effects of various geometry parameters including straight and wavy CNT on the macroscopic stiffness and microscopic stresses of the composites are presented. Numerical results of macroscopic stiffness are compared with previous results obtained from the Halpin-Tsai equations, Mori-Tanaka method, which proves that the present method is valid and efficient.

References

1) Andrews R. and Weisenberger M.C., "Carbon nanotube polymer composites", Current Opinion in Solid State & Materials Science, 2003, pp. 31-37.
2) Halpin J.C. and Kardos, J.L. The Halpin-Tsai Equations: A Review. Polym Eng Sci 1976; 16:344-352.
3) Thostenson E.T. and Chou T.W., " On the elastic properties of carbon nanotube-based composites: modeling and characterization", J. Physics D, 2003, pp. 573-582.
4) Mori T. and Tanaka, K., "Average stress in matrix and average elastic energy of materials with misfitting inclusions", Acta Metallurgica, 1973, pp. 571-574.
5) Weng G.J., "Some elastic properties of reinforced solids, with special reference to isotropic ones containing spherical inclusions", Int J Engng Sci, 1984, pp. 845-856.
6) Wang J. and Pyrz R., "Prediction of the overall moduli of layered silicate–reinforced nanocomposites-Part I: basic theory and formulas", Composites Science and Technology, 2004, pp. 925-34.
7) Fisher F.T., Bradshaw R.D. and Brinson L.C., "Fiber waviness in nanotube-reinforced polymer composites-I: Molulus predictions using effective nanotube properties"", Composites Science and Technology, 2003, pp. 1689-1703.
8) Gao X.L. and Li K., "A shear-lag model for carbon nanotube-reinforced polymer composites", International Journal of Solids and Structures, 2005, pp. 1649-67.
9) Nemat-Nasser S. and Hori M., Micromechanics: Overall Properties of Heterogeneous Materials, London: North-Holland,1993.
10) Benssousan A., Lions J.L. and Papanicoulau G.., Asymptotic Analysis for Periodic Structures, Amsterdam: North-Holland, 1978.
11) Chen X.L. and Liu Y.J., "Square represenrative volume elements for evaluating the effective material properties of carbon nanotube-based composites", Computational Materials Science, 2004, pp. 1-11.
12) Xia Z., Zhang Y. and Ellyin F., "A unified periodical boundary conditions for representative volume elements of composites and applications", Int J Solids Structures, 2003, pp. 1907-1921.
13) Odegard G.M., Gates T.S., Wise K.E., Park C. and Siochi E.J., "Constitutive modeling of nanotube-reinforced polymer composites", Composites Science and Technology, 2003, pp.1671-87.